

Influence of Inlet Air Temperature and its Effects on Combustion using Liquid Fuel Combustion in Taper Can Gas Turbine Combustor

D. R. Srinivasan^a

^a Assistant Professor, Dept. of Mechanical Engg., JNTUA College of Engineering, Anantapur, A.P., India.
Email:- drsrinivasan.mech@jntua.ac.in

Article History: Received: 11 January 2021; Revised: 12 February 2021; Accepted: 27 March 2021; Published online: 4 June 2021

Abstract: The extent of vaporization droplets of liquid fuel that are sprayed into air stream of turbulent swirling flow in a can gas turbine combustor appears to have a very high influence on combustion and emissions thereby performance of the combustor. The investigations containing both experimental as well as numerical in nature was carried out earlier researchers to enhance the fuel vaporization. In this paper a new method is proposed to predict the effects of inlet air temperature on combustion characteristics simulated using a taper can type combustion chamber. A sector of this can type combustor was modelled having an included angle of 51.42° and simulated for combustion process using CFD code star-CD with inlet air temperature entering the combustor after compression varied from 500 K to 1000 K. The turbulence model used in this simulation was model along with high Reynolds number by selecting standard wall treatment. Non-premixed type of combustion method was used for simulation of combustion in the combustion chamber by selecting eddy break-up model called Magnussen's (EBU). The tracking of atomised fuel droplets was done by selecting Lagrangian multiphase model as it contains two phases i.e. liquid fuel droplets injected into turbulent swirling air stream inside the combustion chamber. Reitz Diwakar model was used as droplet breakup model selected and Bai's model was used for droplets of fuel colliding with the wall. Rosin-Rammler method for classifying droplet diameters and probability density functions. All peripheral boundaries of combustion chamber was taken as adiabatic in nature. All sector walls separated by 51.42° were imposed with Symmetry boundary conditions. A well-defined three step reaction model was adopted as combustion reaction that involves liquid fuel as energy source and oxidiser as oxygen with end products of combustion as water vapour and carbon dioxide. As part of grid independency check the model was meshed. Every meshed model has as specified cell size that commences from 3mm to 8mm having step size of 1 mm. The results obtained from meshed models of 3mm and 4mm cell sizes were replicating each other. For less computational time 4mm cell size was used to carry out the investigations. Different cases were run for many inlet air temperatures starting from 500 K to 1000 K with an increase of 100 K in each step size. The results thus obtained were displayed as centre section contour plots of temperature, turbulent kinetic energy drawn along the axial direction till the exit of combustor. The values obtained at the outlet of combustor are the average values and graphical in nature. From this analysis, the inlet air temperature had played pivotal role resulting in enhanced liquid fuel droplets evaporation and combustion in the combustion chamber.

Keywords: turbulent swirling flow, Computational Fluid Dynamics, penetration, vaporization, combustion, inlet air temperature

1. Introduction

The key factors influencing the combustion rate occurring in combustor of the gas turbine is the temperature of the inlet air. Numerous investigations have been carried out by several researchers over years to assess the main effects regarding inlet air temperature upon fuel droplets combustion. The role of liquid fuel vaporization is crucial in combustion, which depends mainly on the temperature prevailing in the engine cylinder region. Liquid fuel vaporization has been observed to be lower at inlet air temperatures as the vaporization process is an exothermic process and the further initiation of combustion does not occur easily.

Increased air temperature intake increases the fuel vaporization rate which accelerates combustion initiation. It was noticed that the gas turbine size was higher leading to increased initial costs and greater operating and maintenance costs. So inlet air temperature is one of the important parameters for fuel vaporization, combustion and its effects are to be predicted.

2. Literature Survey

A great amount of research on separated flow model comprises of specified rate of exchange of mass, conservation of momentum between two phases - liquid and gas phases - are available in a literature on liquid fuel combustion. The separated flow analysis, as described by Crowe et al.[1], was implemented with the Particle-Source-In-Cell (PSIC) method. This process involves dividing the complete spray into a representative category of droplets, with a limited number, and their movement was tracked in the flow field by using Lagrangian method, while the Eulerian method was used for solving conservation equations in the gas phase. Different methods of flow model was proposed by Williams[2] called as Statistical or Continuous Droplet Model (CDM). The formulated the droplets spray by using was modelled according to its approach by adopting conservation equations through statistic distribution function for temperature, speed, droplet diameter, position, multi-dimensional space of time etc. This is a complex differential equation with its solution determined to be highly

expensive in terms of both computing time and also computer storage until some assumptions were made to simplify the equations like no slip exists between gas and droplets phases. This model was applied by Westbrook [3], Ganesan and Spalding [4]. One of the other methods for modelling of spray is using a separately flow method that requires adopting of both liquid phase and gas phase are simultaneously formulated by using conservation equations (CFM). The motion of both fuel and gas droplets were interpreted as a continuum and the two phases were solved by using the concept of Eulerian frame. This technique has been used by Mostafa and Elghobashi[5], Mostafa and Mongia[6] to analyze turbulent jets with droplet vaporizations. After their investigations they modified the analysis by adopting simpler theory such as constant temperature fluid flow and constant temperature of droplets. This approach was proposed by Hallman[7] for investigation of turbulent spray of evaporating droplets with heating. In forecasting spray behavior, Sirignano[8] defined the suitability of variety of formulating methods, emphasized usage of statistical method in the spray analysis.

Three separate cooling methods in the inlet air viz were compared by Farzaneh-Gord et al.[9]. Mechanical chiller freezing, evaporative cooling and also new cooling approaches were introduced by using turbo expanders as compared to traditional methods. It has enhanced the performance of gas turbine by using turbo expanders resulting in better power output and thereby reduction in payback time. Al-Ibrahim et al. [10] studied the various techniques used to cool the inlet air in the gas turbine to improve the power generating rate. Three different approaches were found to provide a better solution, such as high-pressure fogging in the inlet, evaporative cooling and cooling with chilled water. However, using evaporative cooling involves huge amounts of high pressure water, a large amount of power is needed for inlet fogging. It was then found that the best option possible is by choosing refrigerant cooling with chilled water is to achieve minimum inlet temperatures with an advantage of lower power consumption and also lower storage volume requirements.

Amell et al. [11] performed investigation to predict the effect of air cooling at inlet and reported the net output of power varied directly to the entering air mass flow rate. Also, increase in temperature of inlet air had resulted in a reduction in mass flow rate. Ibrahim et al. [12] reported that rise in temperature by 1 °C of air at compressor entry had lowered the combustor performance by 1 percent. The works on spray combustion using separated flow model with specified mass exchange rate, conservation of momentum, energy between two phases i.e. fluid & gas phases published by previous researchers are quite large. In the gas turbine combustion chamber, several scientists have concentrated on numerical flow field calculations. Simulations of strongly swirling flows were carried out in order to improve flame stability by developing toroidal recirculation zones in the combustion chamber's core, resulting in proper fuel mixing, increased fuel evaporation, and a shorter combustor length. Owing to the presence of high turbulence in the fluid, the traditional $k-\epsilon$ turbulence model also called as standard $k-\epsilon$ turbulence model is used for the majority of simulations pertaining to applications in gas turbines. However, the results show that when the traditional $k-\epsilon$ turbulence model with re-circulating swirling flow field was chosen, predictions in some regions were found to be sub-standard. According to Leschziner and Rodi[13], the results obtained from the numerical analysis were in good agreement with the experimental values for a strongly swirling jet when traditional $k-\epsilon$ turbulence model was used. But under reporting was found in the cases of weak swirling jets about the swirl influences in the flow field thereby necessitating corrections to be made. It was and observed that non-inclusion of additional turbulence generated by streamline curvature and anisotropic viscosity in traditional $k-\epsilon$ turbulence model were the reasons for under reporting. Many researchers like Launder et al. [14], Rodi [15], Srinivasan and Mongia [16], Chen and Chang [17] etc. have suggested changes to the standard $k-\epsilon$ model for better results. However, it was noted that neither variant of the proposed modifications has reported consistent results for swirling flow fields with wide range intensities from lower to higher ones. Another approach is the use higher order turbulence models such as the Algebraic Stress Model (ASM) Reynolds Stress Model (RSM). Sturgess and Syed[18] reported that using ASM to simulate flow fields in swirling recirculation flows in the combustion chamber was not as effective as using traditional $k-\epsilon$ turbulence model. The ASM was not suitable for investigating swirling recirculating flows in the central toroidal recirculating region, according to Nikjooy and Mongia[19].

The results from RSM were observed to be sufficient to replicate prominent fluid flow features as reported by Fu et al.[20], Jones and Pascau[21] and Nikjooy and Mongia[19]. However, the complexity of RSM computations and time usage was quite large. Ramos [22] performed numerical analysis for a swirl stabilized gas turbine combustion chamber using standard $k-\epsilon$ model and reported that consideration of scalar viscosity for freely flowing and confined flows was not considered. The predictions of swirling flow fields in different configurations of combustion chamber in gas turbines was made by Rhode et al. [23] Chattree et al. [24], Shyy et al. [25] and McGuiirk and Palma [26] by using standard $k-\epsilon$ turbulence model for turbulence estimation. These investigations offered insight into flow fields in the gas turbine combustion chamber having distinctively recirculation zones with higher level of precision in predicting the recirculation zones. The modeling of reacting flows requires liquid fuel within the combustion chamber for simulating the combustion of liquid fuel spray consideration. Onuma and Ogasawara[27] have demonstrated that liquid fuel droplets in the flames does not burn individually within

envelope flame but they burn with fuel vapor formed by generation due to the evaporation of droplet surface that burns as gaseous diffusion flame. Semibo et al. [28] have used the simplified Nukiyama-Tanasawa equation in prediction of distribution of fuel droplet sizes. They introduced a new theory called Sauter Mean Diameter (SMD) resulting in new distribution function. The results with this method were better in estimation of droplet size distributions in particular for two phase flows.. Stauch et al.[29] analysed the role of operating parameters on ignition delay such as gas phase temperature, droplet temperature, ambient gas pressure and the droplet velocity by using n-heptane as fuel. It was noticed that delay time in ignition relied on the surrounding gas temperature and was not based on droplet velocity. Su et al. [30] carried out an analysis of the combustion performance effects of fuel spray characteristics of gas turbine on parameters such as overall temperature distribution factor and combustion efficiency. The variation in the fuel injection rate, the fuel injection angle and the droplet mean diameter were carried out independently. It was found that rise in fuel injection velocity had improved the overall temperature distribution factor with a small change in combustion efficiency. Movahednejad etc.[31] used the maximum entropy principle (MEP) to determine the size of droplet distributions and droplet velocity at the end of the primary breakup zone. The formulation is based on mass, momentum, and energy conservation principles.

Robert Aftel[32] investigated the effects on fuel droplet atomization properties in the stream of air assisted atomizer. The oxygen existing in the spray gas was found to play a pivotal role in droplets generation and combustion. Some of the operating parameters like atmospheric gas, velocity, temperature, were taken as constant and also neglecting ambient air cooling by fuel droplets evaporation and entrainment effects. by many researchers were and along with training results, were preserved continuously and that the environmental gases were ignored by spray cooling. Bracco [38] used this type of model to check on the sprays of oxygen ethanol droplet combustion in a rocket- engine possessing area of cross-section which is constant. Bracco [36] has used this type of model to analyse droplet fuel spray combustion by using ethanol as fuel and oxygen as oxidiser in a cross-sectional rocket engine. Som [37] had studied the effects of atomized fuel spray evaporation and subsequently entropy generation. Ghosh and Natarajan [38] presented a similar result after identical investigation. The fluid dynamics among the liquid phase and gas phase were considered in one-dimensional models and difficulties in scattering of droplets in stream of turbulent air were excluded. Faeth [39] said one dimensional models are far reaching but they require a certain degree of empiricism. Investigations were carried out by different researchers like Thring and Newby [40], Faeth [41], Khalil and Whitelaw[42], Khalil et.al[43] on the spray flame, burning rate with homogenous flow model as reference and ignoring the slip between two phases i.e. carrier phase and dispersed phase. Further thermodynamic equilibrium and dynamic equilibrium pertaining to every point in the fluid flow field in two phases were presumed to be in phase equilibrium, having same temperature and same velocity. The report by Faeth[41] using model called homogeneous flow was found to overestimate the droplet dispersion in the gaseous phase.

A certain amount of fuel is pumped and sprayed into the stream in the majority of applications, which are denser in nature. As a result, Chiu & Liu[42] introduced the hypothesis of dense fuel sprays in internal combustion engines and industrial furnaces that use a droplet cloud for group combustion of droplets. According to this theory, Chiu and Liu [44], Chiu et al. [45], Chiu and Croke [46], Chiu et al. [47], Kim and Chiu [48], and others investigated the group behaviour of all droplets present in a liquid fuel spray, resulting in the creation of a rich fuel oxidiser mixture in the liquid fuel spray core region. It was noticed that combustion did not occur in the core region due to low air penetration. Also the movement of gaseous fuel in radial direction takes place only by both diffusion and convection that had resulted in inflammable mixture formation in the region which is at some distance in spray axis. By using a simultaneous study of the heterogeneous inner region and the peripheral homogeneous gas phase region, group combustion models are used to predict the behaviour of all droplets.

3.Methodology

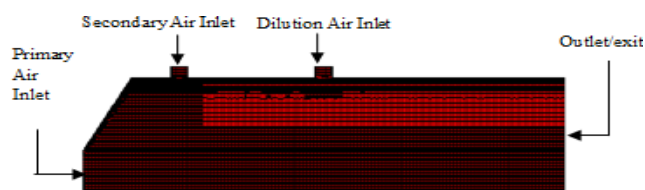
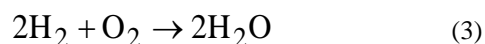


Figure 1. Gas turbine combustion chamber meshed model

For simulation the CFD code used is Star-CD. The domain was modelled, split to total of 7 segments for 360° as an axis-symmetric model and each sector model has 162 137 cells with an angle of 51.42° as described in figure 1. The combustion chamber has three air inlets from which air is supplied comprising of primary inlet in the axial direction. The remaining other inlets are aligned in radial direction referred as secondary and radial dilution air

inlets. All exterior boundaries were assumed to be adiabatic. The domain considered for investigation is 51.42° sector and all sectoral boundaries were assumed to be symmetrical. The walls separating each sector was taken as symmetric in nature. At a pressure of 1 bar, the air enters the combustion chamber and standard k-ε turbulence model was used as turbulence model for wall treatment. The thermal model comprises of both static enthalpy and chemical-thermal option as combustion reaction occurs in the combustion chamber. The eddy break-up (EBU) model presented by Magnussen was chosen because fuel and air enter the combustor separately and it is a non-premixed reaction. The resulting oxidation reaction reactants, n-dodecane as fuel and oxygen as oxidiser, are known as combustion with desired products as water and carbon dioxide. The process is represented as equations (1) to (3) represents the three-step formulation reaction.



The combustion initiation involves a specified layer of cells along the circumference of combustor having 1338 called as ignition cells and they were used to initiate combustion for a limited number of iterations i.e. 100 iterations. After initiation of combustion some undesirable products called named as emissions are generated during the fuel combustion process in addition to the desired formation of carbon dioxide and water vapor. The thermal active nitric oxide model has been chosen to monitor the emissions as a standard function. In addition to this user sub-routines under the name switches and constants were enabled to track both NO_x and also Soot particles. In order to determine Thermal NO_x it is defined as 3-step Zeldovich mechanism shown in Equation (4) to (6).



here K₁, K₂ and K₃ are constants.

The rate constants were calculated based on computational studies [50 - 52]; Baulch et.al [53] had collected and analysed the data required from these tests. They proposed methods to determine the rate of reaction coefficients (Eq.(4) to (6)).

$$\text{K}_1 = 1.8 \times 10^{11} \exp\left(\frac{-38370}{T}\right) \quad \text{m}^3(\text{kgmol})^{-1}\text{s}^{-1} \quad (7)$$

$$\text{K}_{-1} = 3.8 \times 10^{10} \exp\left(\frac{-425}{T}\right) \quad (8)$$

$$\text{K}_2 = 1.8 \times 10^7 T \exp\left(\frac{-4680}{T}\right) \quad (9)$$

$$\text{K}_{-2} = 3.8 \times 10^6 T \exp\left(\frac{-20820}{T}\right) \quad (10)$$

$$K_3 = 7.1 \times 10^{10} \exp\left(\frac{-450}{T}\right) \quad (11)$$

$$K_{-3} = 1.7 \times 10^{11} \exp\left(\frac{-24560}{T}\right) \quad (12)$$

where K_1 , K_2 and K_3 are forward rate constants and where K_{-1} , K_{-2} and K_{-3} are reverse rates constants (Eq.(7) to (12)). The rate of NOx formation is higher at high temperatures because thermal nitrogen fixation involves the splitting of a very strong nitrogen bond. This effect is indicated by high energy activation reaction equation (4), illustrating that this reaction is a rate-limiting stage in the Zeldovich process. Since the activation energy required for the oxidation of nitrogen is low, a near steady state (quasi-state) can be generated. On this basis, the rate of NOx formation at any given time is:

$$\hat{R} = \frac{\rho^2}{1 + K_{-1} \frac{Y_{NO}}{M_{NO}}} \left(K_2 \frac{Y_{O_2}}{M_{O_2}} + K_3 \frac{Y_{OH}}{M_{OH}} \right) \text{ kgmol m}^{-3} \text{ s}^{-1} \quad (13)$$

$$\left[2K_1 \frac{Y_O}{M_O} \frac{Y_{N_2}}{M_{N_2}} - \frac{2K_{-1} \frac{Y_{NO}}{M_{NO}}}{K_2 \frac{Y_{O_2}}{M_{O_2}} + K_3 \frac{Y_{OH}}{M_{OH}}} \right]$$

$$\left(K_{-2} \frac{Y_O}{M_O} \frac{Y_{NO}}{M_{NO}} + K_{-3} \frac{Y_H}{M_H} \frac{Y_{NO}}{M_{NO}} \right)$$

The radicals O, OH and H concentrations were determined using the combustion model embedded into the NOx model. Based on various theories and assumptions including Westenberg [54] the concentration of O atom at equilibrium is calculated from:

$$[O] = K_p [O_2]^{1/2} \text{ kgmol m}^{-3} \quad (14)$$

$$Y_O = [O] \frac{M_O}{\rho} \quad (15)$$

Where

$$K_p = \frac{1.255 \times 10^{-4}}{T^{1/2}} \exp\left(\frac{-31090}{T}\right) \text{ (kgmol)}^{1/2} \text{ m}^{-3/2} \quad (16)$$

the O atoms concentration can be calculated from equation (14) whereas OH and H are initialised to zero.

The soot modeling has been stated and monitored four methods as mentioned below

- PI Scale — Scaling factor for particle inception rate
- SG Scale — Scaling factor for surface growth rate
- OX Scale — Scaling factor for oxidation rate.
- FR Scale — Scaling factor for fragmentation rate

The transport equation for soot mass fraction is given by

$$\frac{\partial}{\partial t} (\rho Y_s) + \frac{\partial}{\partial x_j} (\rho u_j Y_s) = \frac{\partial}{\partial x_j} \left(\frac{\mu_t}{Sc_{t,s}} \frac{\partial Y_s}{\partial x_j} \right) + \rho_s \bar{\omega}_v \quad (17)$$

where Y_s is the soot mass fraction

soot density ρ_s is 1860 kg/m³.

The source term for soot volume fraction is given by

$$\bar{\omega}_v = \bar{\omega}_v, \text{particleinception} + f_v \left(\begin{matrix} \bar{\omega}_v, \text{surfacegrowth} \\ -\bar{\omega}_v, \text{fragmentation} - \bar{\omega}_v, \text{oxidation} \end{matrix} \right) \tag{18}$$

where $f_v = \rho Y_s / \rho_s$ is the mean soot volume fraction.

The mean source terms are referred from collection of flamelets called flamelet library. These was based on the combustion solution containing two opposite reacting streams, taking 973 reactions into account and also 121 fuel species as n-dodecane. The temperature of the fuel jet has also been fixed to 350 K, the temperature of the oxidizer jet has been set to 600 K and entering air pressure at 1 bar. The resultant mean values were determined by integrating probability density function over the space:

$$\bar{\omega}_{v,i} = \alpha_i \int_0^1 \int_0^1 \frac{1}{f_v} \left(\frac{\partial f_{v,i}}{\partial t}(\hat{f}, \hat{\chi}) \right) P(\hat{f}, \hat{\chi}) \hat{f} \hat{\chi} ; i = \text{sg, fr, ox} \tag{19}$$

Where χ is the dispersion rate of the scalar. In the above equation, sg is a surface growth, fr is fragmentation, ox is an oxidation and corresponding scaling factors. This facilitates the user to vary the rates for sensitivity studies by either increase or minimize based on the requirements or to perform calibration tests. In addition

$$\bar{\omega}_{v,pi} = \alpha_{pi} \int_0^1 \int_0^1 \frac{1}{f_v} \left(\frac{\partial f_{v,pi}}{\partial t}(\hat{f}, \hat{\chi}) \right) P(\hat{f}, \hat{\chi}) \hat{f} \hat{\chi} ; i = \text{sg, fr, ox} \tag{20}$$

where pi represents inception of particle and it is the matching scaling factor. The probability density function as described above is given by $P(\hat{f}, \hat{\chi}) = P(\hat{f})P(\hat{\chi})$, by treating them as statistically independent. A β function, equation (20) has been assumed for $P(\hat{f})$. In the current work, $P(\hat{\chi})$ is called as delta function.

$$P(f) = \frac{f^{a-1}(1-f)^{b-1}}{\int_0^1 f^{a-1}(1-f)^{b-1} df} \tag{21}$$

Where $a = \frac{\bar{f}}{g_f} [\bar{f}(1-\bar{f}) - g_f]$

$$b = \frac{(1-\bar{f})}{\bar{f}} a$$

The values of β function are determined using two using two parameters, a and b, from the mean mixture fraction \hat{f} and the corresponding variance g_f that can be defined as

$$g_f = \overline{(f - \bar{f})^2}$$

Two parameters were solved using transport equations to calculate the probability density function. The standard equation used for the mean mixture fraction is \bar{f} and for the variance is g_f

For calculation of probability density function, two parameters using transport equations were solved. the standard equation for the mean mixture fraction is \bar{f} , variance is g_f

$$\frac{\partial}{\partial t}(\rho g_f) + \frac{\partial}{\partial x_j} \left[\rho u_j g_f - \left(\rho D_g + \frac{\mu_t}{\sigma_g} \right) \frac{\partial g_f}{\partial x_j} \right] = 2 \frac{\mu_t}{\sigma_g} \left(\frac{\partial \bar{f}}{\partial x_j} \right)^2 - C_D \rho \frac{\varepsilon}{k} g_f \quad (22)$$

where σ_g is called turbulent Schmidt number

C_D is called coefficient with default values ranging from 0.9 and 2.0, respectively.

The Lagrangian multiphase model was opted to predict the movement of fuel droplets as both the liquid and the gas phases were present in the combustor. The droplet parcels injected in the combustion chamber were specified as 25000. The governing equations such as species concentration, continuity, energy, momentum was solved. After fuel injection these droplets break and correspondingly Reitz-Diwakar model was chosen and for droplet wall interactions Bai's model was found to be most suitable along with boiling option to consider any droplets adhering to the combustor wall.

There are two ways that the fuel droplets that strike the wall and get evaporated. The temperature of the fuel droplets in the first method is higher than the evaporation temperature, while the boiling temperature is influenced by saturation pressure in the second method.

The fuel used for the investigation is n-dodecane which is sprayed in the combustor with fuel air ratio taken as 1:100. The Rosin-Rammler method was chosen to describe the droplet size and density functions that were calculated using parameters such as $X = 4.1E^{-05}$ and $q = 2.5$. With a velocity of 13.25 m/s, fuel injection velocity of 25 m/s, mass air flow of $1.428 E^{-02}$ kg/sec and fuel flow rate of $1.428 E^{-05}$ kg/sec, 2500 fuel droplet parcels were allocated at each injection point, the air enters the combustor through three separate inlets. The model was tested for grid dependency with mesh cell sizes ranging from 3mm to 8mm and 1mm increments. The findings were nearly similar in nature for cell sizes of 3mm and 4mm. Thus, 4 mm of cell was taken for testing because the time requirements of computation are smaller than 3mm. At the entrance of combustion chamber multiple points of fuel injection are chosen at various locations. The last step, the meshed model is simulated and tested for convergence by limiting the iterations as reported by Srinivasan et al.[55, 56].

4.Validation Of Model

For validation of model the following operating parameters were taken as constant and details are given below. Inlet air Swirl 0.37, fuel air ratio 1:100 inlet air temperature 600 K, fuel droplet size $123\mu\text{m}$, air mass flow rate 0.1 kg/sec. fuel injection angle 15° , injected fuel temperature 350 K and the case was run with these parameters. The outcome of the analysis was compared with findings as given below.

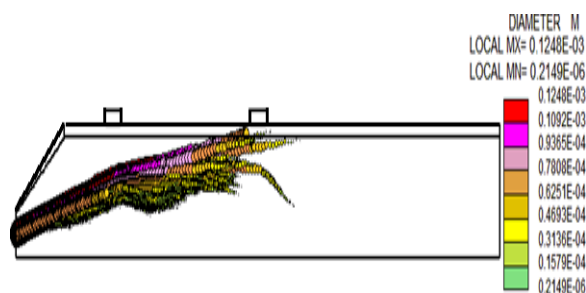


Figure 2. Penetration of droplets with initial diameter of droplets $123\mu\text{m}$

From the figure 2 it can be noticed that presence of fuel droplets with diameter of $123\mu\text{m}$ were located beyond 2.25 (Z/D) where Z is represented as combustor length and D is represented as diameter of combustor which is obtained from the analysis thereby replicating the results as reported by Sharma et al [56] in literature shown in figure 3 and figure 4.

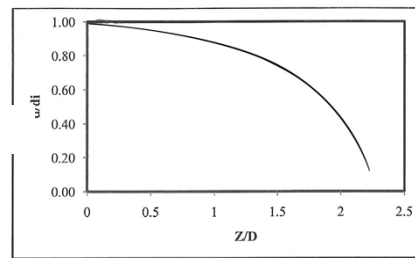


Figure 3. Penetration of droplets obtained in the combustor for droplet diameter of 123µm

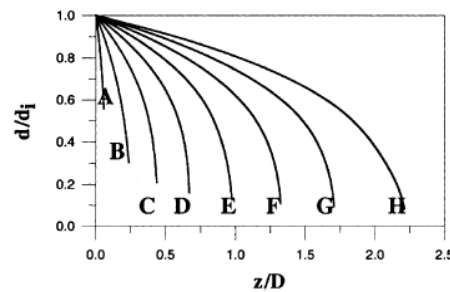


Figure 4. Penetration of different droplets represented by classes in the combustor

Table 1 Classification of droplet diameters

Droplet Classes	A	B	C	D	E	F	G	H
Size µm	8	3	8	3	8	3	08	23

5. Results & Discussions

Analysis was carried out to determine the role of operating parameters including turbulence kinetic energy average temperature, with a change of temperature at inlet. Some of parameters that were kept constant in the present investigation and the details are as follows: Air swirl at inlet 0.37, fuel air ratio 1:100, density of air at inlet 0.5087 kg/m³ air mass flow rate 0.1 kg/sec, fuel injection angle 15°. The inlet air temperature was initially taken as 500K and raised by 100K for subsequent iterations till 1000K. The results obtained from the analysis are presented as temperature contour plots and turbulent kinetic energy contour plots.

5.1 Temperature Contour Plots

The contour plots show temperature variations reflected by areas occupied by different regions at various locations in the combustor. Figure 5 depicts the temperature that occurs in the combustor along its length for various inlet air temperatures of 500K, 600K, 700K, 800K, 900K, and 1000K as contour plots.

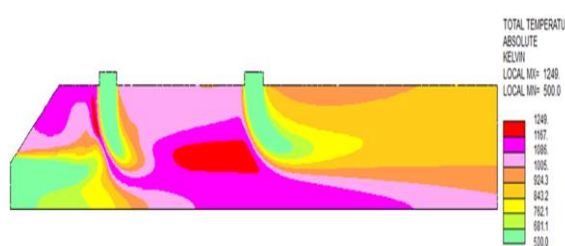


Fig.5.1(a)

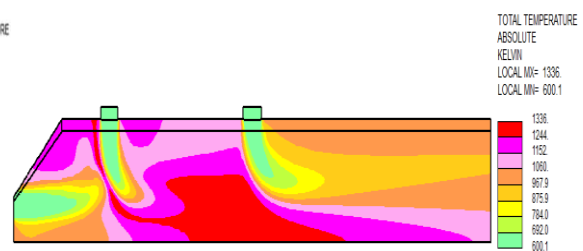


Fig.5.1(b)

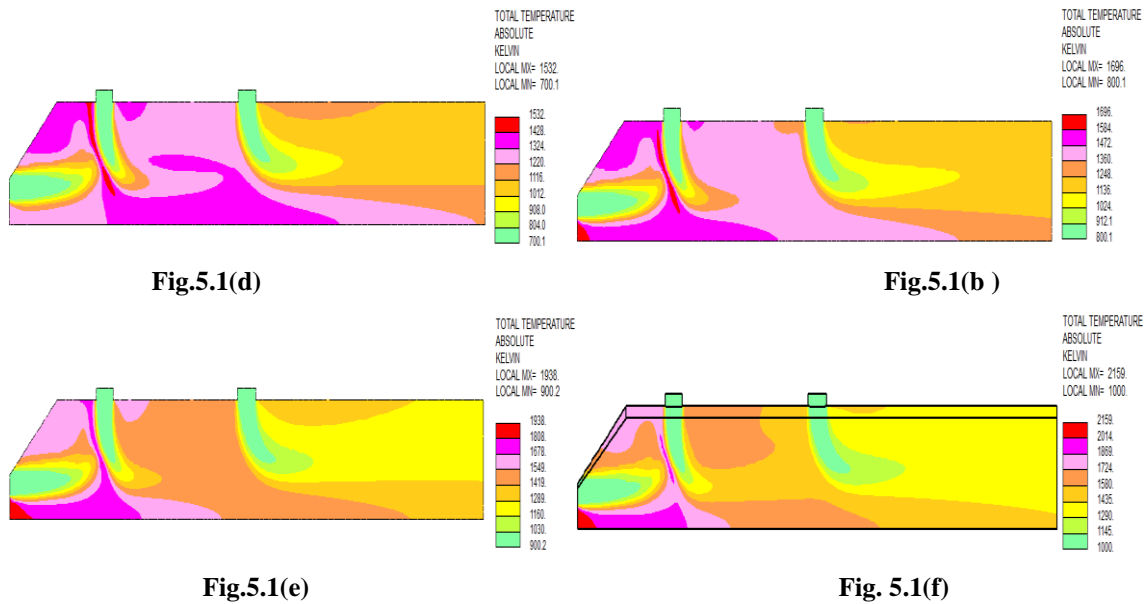


Fig. 5.1(a) to Fig. 5.1(f) Temperature contour plots for different inlet air temperatures.

Figure 5.1 (a) to figure 5.1(f) provides the information about the role of inlet air temperature from 500K to 1000K increased by 100K and corresponding changes in temperature at different locations of combustor. The average and maximum temperatures in the combustor tend to rise as the temperature of the inlet air had increased. The average temperatures and maximum temperatures prevailing in the combustor appear to increase with rise in inlet air temperature. In figure 5.1 (a) it is observed that the highest temperature position is initially located between secondary and dilution inlets and gets strengthened in figure 5.1 (b) accompanied with increase in its area. From figure 5.1 (c), figure 5.1 (d) it appears this position appear to get shifted to left of secondary air inlet. For the case of inlet air temperature 900K and 1000K the maximum temperature is identified to be situated at the axial inlet figure 5.1 (e) and figure 5.1 (f) and the regions containing maximum temperature has decreased as seen in figure 5.1 (c) and figure 5.1 (f). Also the difference in various regions of temperatures at the exit after combustion of fuel has decreased as the temperature at the inlet had increased. This can be explained as the rise in the air intake temperature takes place the temperature adjacent to the fuel droplets is elevated and this had resulted in higher energy availability to the atomised fuel droplets for better evaporation and formation of near homogenous mixture.

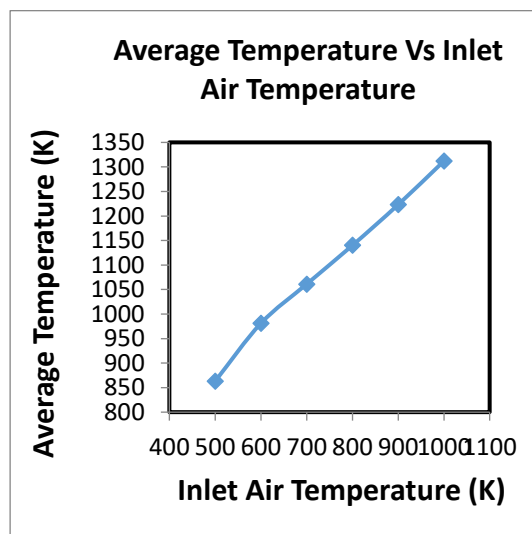


Fig. 5.1(g) Variation of Average temperature with inlet air temperature

The figure can be noticed. 5.1(g) the average temperature appears to rise as the inlet air temperature increases. Also it can be noticed that with a rise in the air inlet temperature, the vaporization rate of atomised fuel droplets injected into the combustion chamber had improved. The average temperature increase rate initially for 500 K is

found to be 363 K, appears to reach a peak value of 381 K, and later decrease significantly with the increase in air intake temperature.

5.2 Turbulent kinetic energy contours

The variation of turbulent kinetic energy are presented in the form of contour that provide information about the areas occupied by various regions and these are located at different positions in the combustor.

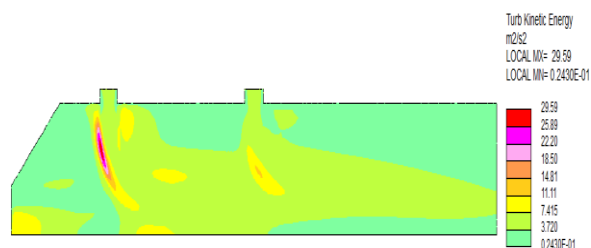


Fig. 5.2(a)

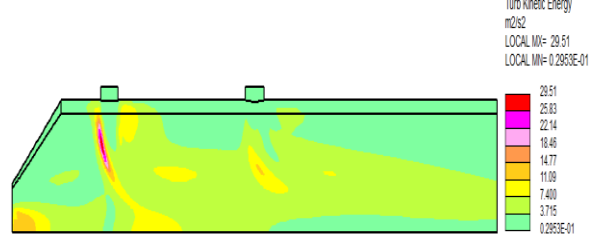


Fig. 5.2(b)

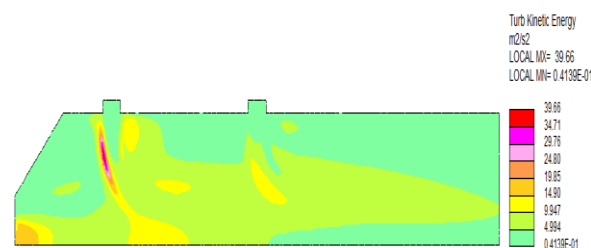


Fig. 5.2(c)

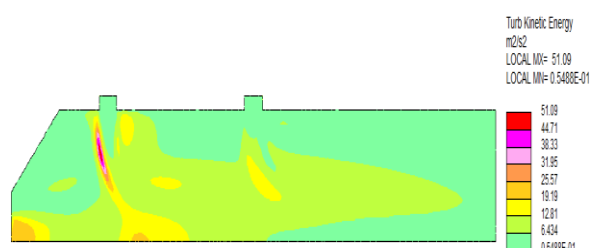


Fig. 5.2(d)

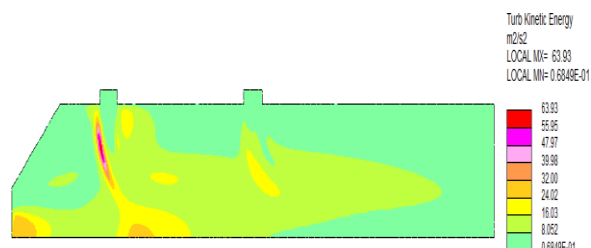


Fig. 5.2(e)

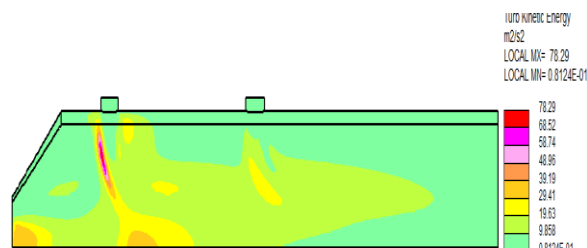


Fig. 5.2(f)

Fig. 5.2(a) to 5.2(g) Turbulent Kinetic Energy contour plots for different inlet air temperatures

It is noted that there is rise in maximum turbulent kinetic energy values, but the areas occupied by these higher values appear to shrink as inlet air temperature had increased. Also, these regions appear to be same near the outlet with increase in temperature. Further it can be justified as This can be explained as the differences in turbulent kinetic energy values had decreased due to effects of combustion induced turbulence become uniform with increase in temperature.

6. Conclusions:

By increasing the inlet air temperatures from 500 K to 1000 K with a 100 K step size, the CFD simulation was used to predict the effect of air temperature at inlet on fuel combustion. Results obtained for different operating parameters with 600 K inlet air temperature have better values.

The temperature contour plots reveal that the maximum value of the temperature is 1336 K, while the average temperature difference computed between the inlet temperature and the outlet temperature was observed to be maximum of 361 K. The turbulent kinetic energy has maximum value of 29.51 m^2/s^2 and this value appears to be moderate. But the areas with highest values have dropped as the inlet temperature was raised. In addition at the outlet the values of turbulent kinetic energy is almost equal in most of the cases.

The analysis thus revealed that the input air temperature of 600 K was best with fuel injection rates of 25 m/s and a fuel injection angle of 15° as it has maximum overall increase of the average temperature, provides a moderate value of turbulent kinetic energy in comparison with other temperature cases.

Reference

1. Crowe, C.T., Sharma, M.P. and Stock, D.E., 1977, The Particle-Source-In-Cell (PSI-Cell) Model for Droplet Sprays, *ASME J. Fluid Engg.*, Vol. 99, p. 325.
2. Williams, F.A., 1962, Progress in Spray Combustion Analysis, Proc. Eight Symp. (Int.) on Combustion, The Comb. Inst., p. 50.
3. Westbrook, C.K., 1976, Three-Dimensional Numerical Modelling of Liquid Sprays, Sixteenth Symp. (Int.) on Combustion, The Comb. Inst., p. 1517.
4. Westbrook, C.K., 1976, Three-Dimensional Numerical Modelling of Liquid Sprays, Sixteenth Symp. (Int.) on Combustion, The Comb. Inst., p. 1517.
5. Mostafa, A.A. and Elghobashi, S.E., 1985, A Two-Equation Turbulence Model for Jet Flows Laden with Vaporizing Droplets, *Int. J. of Multiphase Flow*, Vol. 11, No. 4, p. 515.
6. Mostafa, A.A. and Mongia, H.C., 1987, ON Modelling of Turbulent Evaporating Sprays: Eulerian versus Lagrangian Approach, *Int. J. of Heat and Mass Transfer*, Vol. 30, No. 12, p. 2583.
7. Hallmann, M., Scheurlen, M. and Wittig, S., 1995, Computation of Turbulent Evaporating Sprays: Eulerian versus Lagrangian Approach, *ASME J. of Engg. for Gas Turbine and Power*, Vol. 117, p. 112.
8. Sirignano, W.A., 1986, The formulation of Spray Combustion Models: Resolutions Compared to Droplet Spacing, *ASME J. of Heat Transfer*, Vol. 108, p. 633.
9. Farzaneh-Gord, M.; Deymi-Dashtebayaz, M., 2011, Effect of various inlet air cooling methods on gas turbine performance, *J. of Energy*, Vol. 36, pp. 1196–1205.
10. Al-Ibrahim A. M.; Varnham, A., 2010, A review of inlet air-cooling technologies for enhancing the performance of combustion turbines in Saudi Arabia. *Applied Thermal Engineering*, Vol. 30, pp.1879–1888.
11. Amell, A. A.; Cadavid, F., *Journal of Applied Thermal Engineering*, 22(13), 2002, 1529–1533.
12. Ibrahim, T. K.; Rahman M. M.; Abdalla A. N., *International Journal of Physical Sciences*, 6(11), 2011, 620-627.
13. Leschziner, M.A. and Rodi, W., 1984, Computation of Strongly Swirling Axisymmetric Few Jets, *AIAA J.*, Vol. 22, No. 12, p. 142.
14. Launder, B.E., Priddin, C.H. and Sharme, B.L. 1977, The Calculation of Turbulent Intensity Boundary Layers on Spinning and Curved Surfaces, *ASME J of Fluid Engg.*, Vol. 99, p.231.
15. Rodi, W., 1979, Influence of Buoyancy and Rotation on Equations for the Turbulent Length Scale, Proc. 2nd Smp. On Turbulent Shear Flows, Imperial College, London, p. 10.37.
16. Srinivasan, R. and Mongia, H.C., 1980, Numerical Computations of Swirling Recirculating Flows, Final Report, NASA CR-165196.
17. Chang, K.C. and Chen, C.S., 1993, Development of Hybrid k- ϵ Turbulence Model for Swirling Recirculating Flows under Moderate to Strong Swirl Intensities, *J. Numerical Methods in Fluids*, Vol. 16, p. 421.
18. Sturgess, G.J. and Syed, S.A. 1990, Calculation of Confined Swirling Flows, *Int. J. Turbo Jet Engines*, Vol. 7, p. 103.
19. Nikjooy, M. and Mongia, H.C., 1991, A Second Order Modelling Study of Confined Swirling Flows, *Int. J. of Heat and Fluid Flow*, Vol. 12, p. 12.
20. Fu, S., Huang. P.G., Launder, B.E., and Leschziner, M.A., 1988, A Comparison of Algebraic and Differential Second-Moment Closures for Axi-symmetric Turbulent Shear Flows with and without Swirl, *ASME J. Fluid Engg.*, Vol. 110, p. 216.
21. Jones, W.P. and Pascau, A., 1989, Calculation of Confined Swirling Flows with a Second Moment Closure, *ASME J. Fluid Engg.*, Vol. 111, p. 248.
22. Ramos, J.I, 1985, A Numerical Study of Swirl Stabilized Combustors, *J. Non-Equilib. Thermo.*, Vol. 10, p. 263.
23. Rhode, D.L., Lilley, D.G. and McLaughlin, D.K., 1982, On the Prediction of Swirling Flow-fields found in Axi-symmetric Combustor Geometries, *ASME J. Fluid Engg.*, Vol. 104, p. 378.
24. Chattree, M., Celik, I. and Singh, S., 1987, Analysis of Turbulent Swirling Flow in a Model Combustor, Proc. Of ASME Winter Annual Meeting in Boston, Massashusetts.

25. Shyy, W., Correa, S.M. and Braaten, M.E. 1988, Computations of Flow in a Gas Turbine Combustor, *Comb. Sci. and Tech.*, Vol.58, p. 97.
26. McGuirk, J.J. and Palma, J.M.L.M., 1993, The Flow Inside a Model Gas Turbine Combustion: Calculations, *ASME J. of Engg. for Gas Turbine and Power*, Vol. 115, p. 594.
27. Onuma, Y. and Ogasawara, M., 1974, Studies on the Structure of a Spray Combustion Flame, Fifteenth Symp. (int.) on Combust., *The Comb. Inst.*, p.453.
28. Semibo, V., Andrade, P., Carvalho, M.G., 1996, Spray Characterization: numerical prediction of Sauter mean diameter and droplet size distribution, *Fuel* Volume 75 No. 15 pp. 1707-1714
29. Stauch R., Lipp S., Maas U., 2005, Detailed Numerical Simulation of Droplet Combustion, *Proceedings of the European Combustion Meeting*, pp. 1-6
30. Su K. And Zhou C.Q., Numerical Study of Spray Parametric Effects on Gas Turbine Combustion Performance
31. Movahednejad, E., Ommi, F., and Hosseinalipour, M. S., 2010, Prediction of Droplet Size and Velocity Distribution in Droplet Formation Region of Liquid Spray, *Entropy*, Vol. 12, pp. 1484-1498
32. Aftel, R., Effect of Atomization Gas Properties on Droplet Atomization in an 'Air-Assist' Atomizer in his Thesis, Virginia Polytechnic Institute and State University.
33. Faeth, G.M., 1983, Evaporation and Sprays, *Prog. Energy and Comb. Sci.*, Vol. 9, p. 1.
34. Faeth, G.M., 1987, Mixing, Transport and Combustion of Sprays, *Prog. Energy and Comb. Sci.* Vol. 13, p.293.
35. Nurruzzaman, A.S.M., Siddali, R.G. and Beer, J.M., 1971, The Use of a Simplified Mathematical Model for prediction of Burnout of Non Uniform Sprays, *Chem. Engg. Sci.*, Vol. 26, p. 1635.
36. Chin, J.S., Durret, R. and Leferbvre, A.H., 1984, The Interdependence of Spray Characteristics and Evaporation History of Fuel Sprays, *ASME J. of Engg. for Gas Turbine and Power*, Vol. 106, p. 639.
37. Chin, J.S., Nickolaus, D. and Leferbvre, A.H. 1986, Influence of Down Stream Distance on the Spray Characteristics of Pressure Swirl Atomizers, *ASME J. of Engg. for Gas Turbine and Power*, Vol. 106, p. 219.
38. Bracco, F.V., 1974, Applications of Steady State Spray Equations to Combustion Modelling, *AIAA J.*, Vol. 21, p. 123.
39. Som, S.K., 1986, Evaporation and Entropy Generation Histories of Atomised Spray of Non-Uniform Liquid Droplets in a Stream of Hot Gas, *drying*, 86, Vol. 1, p. 314.
40. Natarajan, R. and Ghosh, A.K., 1975, Velocity Histories of Vaporizing Fuel Droplets moving through Stagnant Gas, *Fuel*, Vol. 54, p. 153.
41. Faeth, G.M., 1977, Current Status of Droplet and Liquid Combustion, *Prog. Energy and Comb. Sci.*, Vol 3, p. 191.
42. Thring, M.W and Newby, M.P., 1953, Combustion Length Enclosed Turbulent Jet Flames, *Fourth Symp. (Int.) on Combust.*, *The Comb. Inst.*, p. 789.
43. Avery, J.F. and Faeth, G.M., 1974, Combustion of Submerged Gaseous Oxidiser Jet in a Liquid Fuel, *Fifteenth Symp. (Int.) on Combustion*, *The Comb. Inst.*, p. 501.
44. Khalil, E.E. and Whitelaw, J.H., 1976, Aerodynamic and Thermodynamic Characteristics of kerosene-Spray Flames, *Sixteenth Symp. (Int.) on Combustion*, *The Comb. Inst.*, p. 135.
45. Khalil, E.E. 1978, A Simplified Approach for the Calculation of Free and Confined Sprays, *AIAA Paper No. 78-029*.
46. Chiu, H.H and Liu, T.M., 1977, Group Combustion of Liquid Droplets, *Comb. Sci. and Tech.* Vol. 17, p. 127.
47. Chiu, H.H., Ahulwalia, R.K., Koh, B. and Croke, E.J., 1978, Spray Group Combustion, *AIAA Paper 78-75*, presented at *AIAA Sixteenth Aerospace Science Meeting*, Huntsville, Ala.
48. Chiu, H.H., and Croke, E.J., 1981, Group Combustion of Liquid Fuel Sprays, *Energy Tech. Lab. Report 81-2*, Univ. of Illinois, Chicago.
49. Chiu, H.H., Kim, H.Y. and Croke, E.J., 1982, Internal Group Combustion of Liquid Droplets, *Nineteenth Symp. (Int.) on Combustion*, *The Comb. Inst.*, p. 971.
50. Kim, H.Y. and Chiu, H.H., 1983, Group Combustion of Liquid Droplet Sprays, *AIAA Paper 83-0150*, presented at *AIAA 21st Aerospace Science Meeting*, Reno, Nevada.

51. M.Y. Abdollahzadeh Jamalabadi, Moein Rajabzadeh, P. Hooshmand, 2015, Effect of Fuel Inject Angle on the Thermal Behavior of a 2D Axisymmetric Non-Premixed Methane–Air Flame in Vertical Cylinder Filled by Porous Media, *International Journal of energy Engineering*, Volume 5, pp. 1-8.
52. Flower, W.L., Hanson, R.K., and Kruger, C.H. 1975. 'Kinetics of the reaction of nitric oxide with hydrogen', 15th Symp. (Int.) on Combustion, The Combustion Institute, pp. 823-832.
53. Monat, J.P., Hanson, R.K., and Kruger, C.H. 1979, Shock tube determination of the rate coefficient for the reaction
54. $N_2 + O \rightarrow NO + O$ ' 17th Symp. (Int.) on Combustion, The Combustion Institute, p. 543-552.
55. Baulch, D.L., Drysdall, D.D., Horne, D.G., and Lloyd, A.C. 1973. *Evaluated Kinetic Data for High Temperature Reactions*. Butterworth.
56. Westenberg, A.A. 1971. 'Kinetics of NO and CO in lean, premixedhydrocarbon-air flames', *Combust. Sci. and Tech.*, 4, pp. 59-64.
57. Srinivasan, D.R., Pandurangadu, V., Gupta, A.V.S.S.K.S., Influence of Liquid Fuel Injection Velocities on Combustion in a taper can gas turbine combustion chamber. *International Journal of Engineering Science and Innovative Technology (IJESIT)* Volume 2, (6), 2013, pp. 167-172.
58. Srinivasan, D.R., Pandurangadu, V., Gupta, A.V.S.S.K.S., 2013, Penetration of Liquid Fuel Droplets for different fuel injection velocities in the taper can gas turbine combustor. *International Journal of Applied Engineering and Technology*, Vol. 3(4), pp. 18-22.
59. Sharma, N.Y., Datta, A. and Som, S.K., 2001, Influence of Spray and Operating Parameters on Penetration of Vaporizing Fuel Droplets in a Gas Turbine Combustor, *Applied Thermal Engineering*, Vol. 21, pp. 1755-1768